

Microwave Optics Experiments

Author: Miguel García Fernández

Facultat de Física, Universitat de Barcelona, Diagonal 645, 08028 Barcelona, Spain.*

Advisor: Cèsar Ferrater Martorell

Abstract: In this project, we use a simple experimental set-up in order to observe Total Internal Reflection within a right-angle PVC prism. Later, we measure Frustrated Total Internal Reflection, also known as optical tunnelling, using two of such prisms. Before doing so, we also study our non-ideal experimental set-up. Its imperfections, on the one hand, set several difficulties when it comes to quantitatively analyze the experimentally obtained data. On the other hand, though, these deviations from the ideal behaviour are interesting enough to be studied by themselves. As suggested in the title, these experiments have been performed using microwaves, instead of visible light, the most commonly used spectrum in optics experiments.

I. INTRODUCTION

According to [1], when an electromagnetic wave propagates from a medium A with refraction index n_A to a medium B with a smaller refraction index n_B , there exists a certain angle of incidence, known as critical angle, for which none of the wave is transmitted, but instead, all of it is reflected. This phenomenon is called Total Internal Reflection (TIR).

If, in such situation, another medium C with refraction index $n_C > n_B$ is placed near enough the interface between A and B , TIR is not observed. Instead, we have Frustrated Total Internal Reflection (FTIR), a phenomenon by means of which part of the wave manages to propagate from A to C , thus *frustrating* total reflection. The fraction of energy that is carried by the transmitted wave (also known as transmittance), according to [3], depends exclusively of the incidence angle, the refraction indexes of the three mediums and the distance between mediums A and C . FTIR is also known as optical tunnelling due to its similarities with the quantum phenomenon of tunnelling.

In this project, we use a simple experimental set-up in order to measure Total Internal Reflection (TIR) and Frustrated TIR (FTIR). Then, we analyze the obtained data and compare it to the expected results. Before doing these two main experiments, a study of the experimental set-up is required.

Some of the figures shown in this document belong to documents [4].

II. EXPERIMENTAL SET-UP

Our experimental set-up consists of the following elements (see also Figure 1):

- A microwave emitter of wavelength $\lambda = 2,86$ cm. It is directional, meaning that there is an axis along which

the emitted field is the greatest. It emits with plane polarization; a goniometric support allows controlling the orientation of the emitted field, which is perpendicular to the axis.

- A microwave detector, which also detects in a directional and polarized way, with a goniometric support that allows to control the polarization. It shows a potential as a response to the intensity (squared amplitude) of the electromagnetic field. The measured potential is in arbitrary units. It has an integrated amplifier that allows us to increase the sensibility of the measures.
- A voltmeter, which we use to accurately read the measures given by the detector.
- A goniometer that allows to set a desired angle between the axes of the emitter and the detector.
- A pair of identical right-angle PVC prisms, with a theoretical refraction index of 1.531, according to [2].
- A set of sheets of different (small) widths. They will be used in FTIR in order to set different distances between the two prisms. Such distances have to be very small, as will be seen later.

III. EXPERIMENTAL RESULTS AND DISCUSSION

A. Study of the emitter

As stated above, the detector measures the intensity of the field. Figure 2 shows the polar distribution of such intensity. What we can conclude from this graph is that the emitted electric field is directional (as stated above), allowing us to talk about a propagation vector or, similarly, a Poynting vector associated to it. Specifically, such vector is the unitary vector in the direction of the axis of the emitter.

*Electronic address: mgarcife42@alumnes.ub.edu

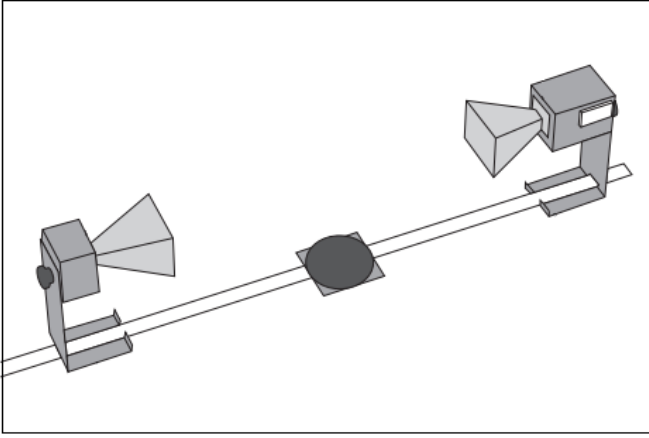


FIG. 1: Emitter, goniometer and detector of our experimental set-up

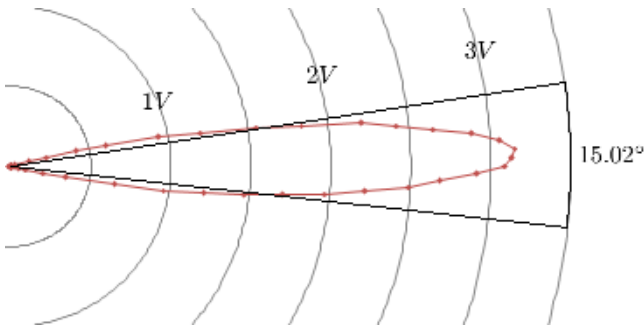


FIG. 2: Polar distribution of the intensity of the emitted field. The angle (15.02°) represents that within which the potential measured by the detector is greater than half the maximum one, obtained when the emitter and the detector are facing each other.

Now, let us show the radial dependence of the intensity. In order to measure it we have chosen the direction of maximum intensity, which in Figure 2 has been seen to be the axis of the emitter.

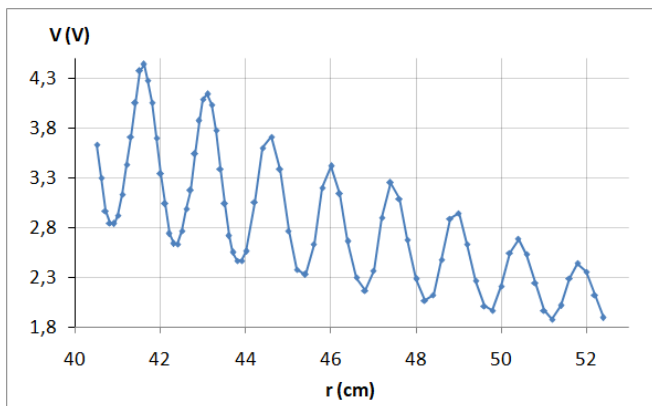


FIG. 3: Potential measured by the detector versus distance between emitter and detector, along the emitter axis.

This was an unexpected result. What one would initially expect is something between constant intensity (associated to plane waves, with a defined directionality such as ours) and a r^{-2} decay (spherical waves, which could be regarded as those generated by a punctual source such as our emitter). Instead, we get a sinusoidal function whose mean value decays with the distance. The sinusoidal behaviour can be regarded as a consequence of the shapes of the receptor and the emitter. Indeed, some of the intensity arriving to the detector is reflected by it, and a fraction of this reflected waves is also reflected in turn by the emitter, and so and so forth. This effect ends up causing the stationary waves shown in Figure 3. This explanation is reinforced by the fact that the wavelength of the function in the figure is around 1.7 cm , similar to the wavelength of our microwaves. On the other hand, the decay of the mean value can be regarded as a consequence of the fact that the emitter is a punctual source. Such decay can be approximated to the spherical one with a relative error of 17%.

Among the several error sources identified throughout experiments, the radial dependence of intensity turned out to be the most important one. We can give an upper bound to this error by measuring the slopes in the figure. Taking the greatest one, we get

$$\varepsilon_r = \frac{4.061V - 3.039V}{42.1\text{cm} - 41.8\text{cm}} \approx 0.34\text{ V/mm}.$$

Further measures have been done taking into account this fact. In order to minimize its effect, we keep the distance between emitter and detector constant, in such a way that we are always placed at one of the relative maximums of Figure 3.

B. Study of the detector

As stated above, the detector measures a potential V as a response to the intensity I of the incident field. A reasonable question to ask ourselves is whether dependence $V(I)$ is linear. This would be difficult to tell without further information of the device. In addition, knowing that the detector works via a rectifying diode, the assumption of linear dependence seems even weaker. Therefore, the understanding of such dependence cannot be achieved without performing further measures.

In order to measure $V(I)$ we take advantage of the fact that we can polarize the field. Then, we can use Malus's law, which states that the transmitted intensity through a polarizer is

$$I = I_0 \cos^2 \alpha,$$

where I_0 is the intensity of the incident field into the polarizer, which is set at an angle α with respect to the plane-polarized wave.

If the response of the detector was linear, we would measure that V varies as $\cos^2 \alpha$. But this is not the case, see Figure 4.

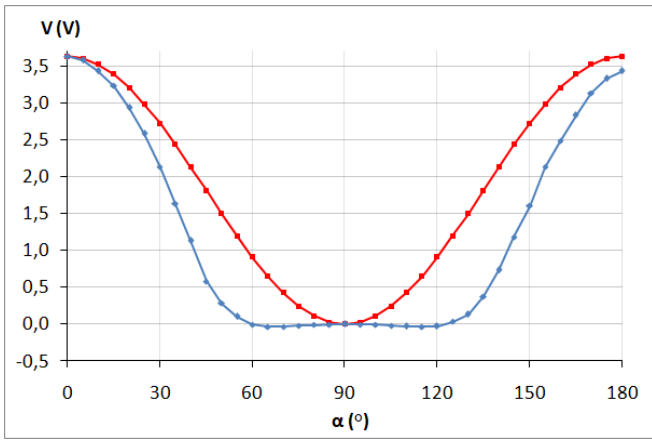


FIG. 4: The red curve, corresponding to Malus’s law, shows the linear response of an hypothetical detector. The blue curve shows the response of our real detector, which is less sensible to lower intensities.

What this graph is telling us is that the response of the detector is better when the incident field has a greater intensity. In fact, the response is very poor when the intensity is below half the maximum intensity.

To compare linear and experimental response we compute their quotient, shown in Figure 5. This allows us to get rid of the arbitrary value of $V(I_0) = 3.6 V$.

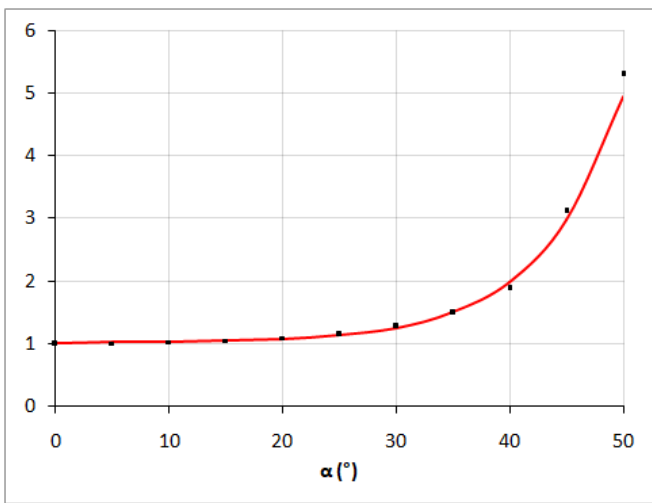


FIG. 5: Quotient of the linear response between the experimental response, in black, up to 50° . The red curve is the most suitable exponential model for this behaviour. The determination coefficient of this approximation is $R^2 = 0.9986$.

Figure 5 also shows that a good approximation for the quotient is an exponential function. This guess turns out to work very well for angles up to 50° (or equivalently for high intensities/potentials). Giving the specific coefficients of this function in this case is pointless, because they may depend on the amplification factor of the detector, and therefore will not be the same in all our ex-

periments.

C. Critical Angle. Total Internal Reflection

Now, we start working with our right-angle, PVC prisms. We set them upon the goniometer, allowing us to measure the angle of incidence of the emitted field into the prisms and the angle of the field transmitted from them.

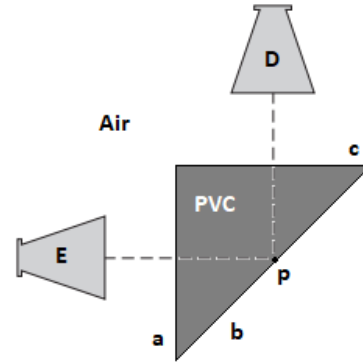


FIG. 6: Floor plan of the set-up chosen to observe TIR. In order to measure this phenomenon, we place a prism upon the goniometer. To measure the incident and transmitted/reflected angles, we need to place the point p of the prism on the center of the goniometer.

TIR is measured for incidence angle 45° at point p , according to Figure 6.

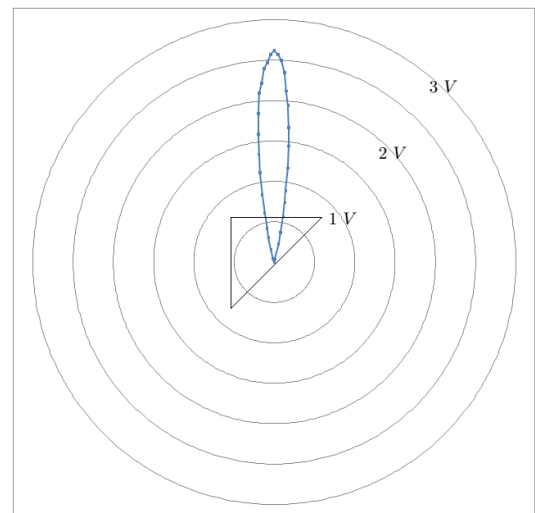


FIG. 7: Polar distribution of the intensity of the detected field. The direction of the beam corresponds to the Poynting vector of the reflected field. Since we do not observe a second beam, corresponding to a transmitted field, we can conclude that TIR is given.

In Figure 7 we see that all the intensity is reflected, since, on one hand, there is only a beam of electromag-

netic waves, and on the other hand, such beam revolves around the direction corresponding to the reflection of the incident beam.

Theoretical critical angle for PVC, assuming $n = 1.531$, is $\theta_c = 40.8^\circ$. Our experimental set-up is not appropriate to obtain an experimental value of such angle. This is because refraction in the interface air-PVC shifts the point of incidence of the beam in the inner surface of the PVC. Therefore, the outgoing beam cannot be measured by the detector, which is always aimed to the center of the goniometer, corresponding to the point p of the prism.

D. Frustrated Total Internal Reflection

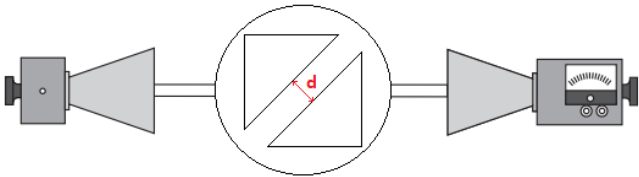


FIG. 8: Experimental set-up used to observe FTIR. According to [1] and [3], when FTIR is produced, the incident and the transmitted angle are the same. Therefore, the simplest way to measure FTIR in our case is making the incident angle equal to 0° (normal incidence), as shown in the figure.

As seen in [3], in the specific case in which the first and the third medium (PVC, in our case) have the same refraction index n , and the intermediate medium has unitary refraction index (air, in our case), the expression of the transmittance is:

$$\frac{1}{T} = \alpha \sinh^2 \gamma + \beta,$$

where γ is defined by

$$\gamma \equiv \frac{2\pi d}{\lambda} \sqrt{n^2 \sin^2 \phi - 1}, \quad (1)$$

with ϕ the angle of incidence, in our case 45° .

The first problem that arises when we try to compare our experimental data to the theoretical curve is that \sinh^2 cannot be analytically linearized. Nevertheless, now one of the main experimental difficulties, which was the fact that the distances between prisms have to be very small in order to observe this phenomena, enables us to compute a good approximation to the FTIR theoretical model. Indeed:

$$\sinh^2 x = \left(\frac{e^x - e^{-x}}{2} \right)^2 = \frac{1}{2} \left(\frac{e^{2x} + e^{-2x}}{2} - 1 \right)$$

Introducing the Taylor series of the exponential functions, it is easy to see that

$$\sinh^2 x = x^2 + o(x^4).$$

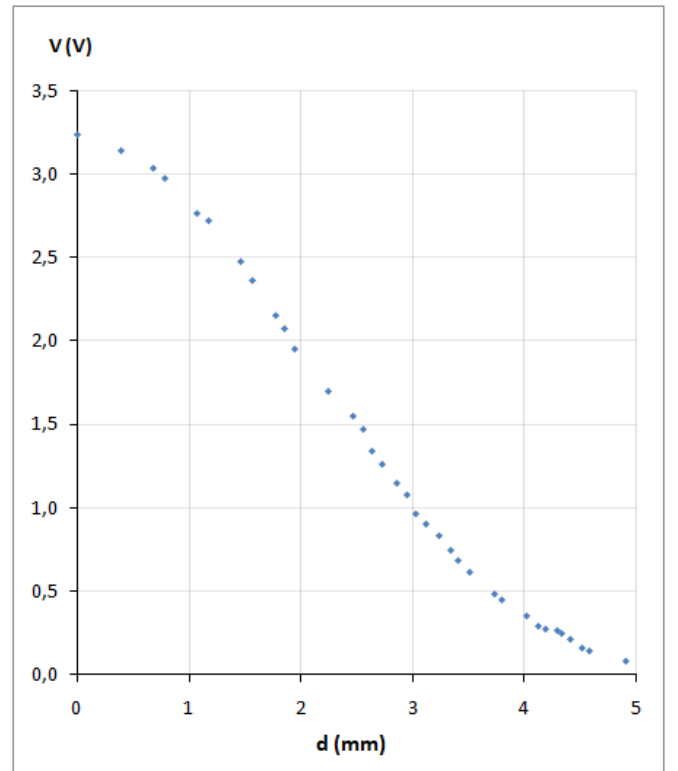


FIG. 9: Potential measured by the detector versus the distance d between the interfaces of the two prisms. As expected, the transmitted intensity decreases as the distance increases. This agrees, qualitatively, with the expected theoretical behaviour.

Therefore, we will be able to use the approximation

$$\sinh^2 x \approx x^2$$

whenever $x^2 \ll 1$. In our case, $x = \gamma$, and the approximation

$$\frac{1}{T} = \alpha \sinh^2 \gamma + \beta \approx \alpha \gamma^2 + \beta \quad (2)$$

will be justified when $\gamma^2 \ll 1$. Specifically, replacing in equation (1) the known values of $\lambda = 28.6 \text{ mm}$, $n = 1.531$ and $\phi = 45^\circ$, we get

$$\gamma = d \cdot 9.1 \cdot 10^{-2} \text{ mm}^{-1} \approx \frac{d}{10.98 \text{ mm}}$$

with d (the distance between prisms, Figure 8) in mm . The quadratic approximation in equation (2) will be valid (with less than a 10% relative error) when

$$\frac{d}{10.98 \text{ mm}} \leq 0.5, \text{ this is, when } d \leq 5.49 \text{ mm}$$

(and therefore, for all of our presented measures), since

$$\left| \frac{\sinh^2 x - x^2}{\sinh^2 x} \right| < 0.1 \quad \forall 0 \leq x \leq 0.5.$$

The second problem that arises when trying to compare theoretical and experimental results is the non-linear response of the detector. Even though we have been able to model the response as an exponential function, we also argued that the specific coefficients of such model may vary between different scales of intensity.

Nevertheless, Figure 5 shows that for angles low enough (which would now correspond to low distances), the response of the detector is almost linear.

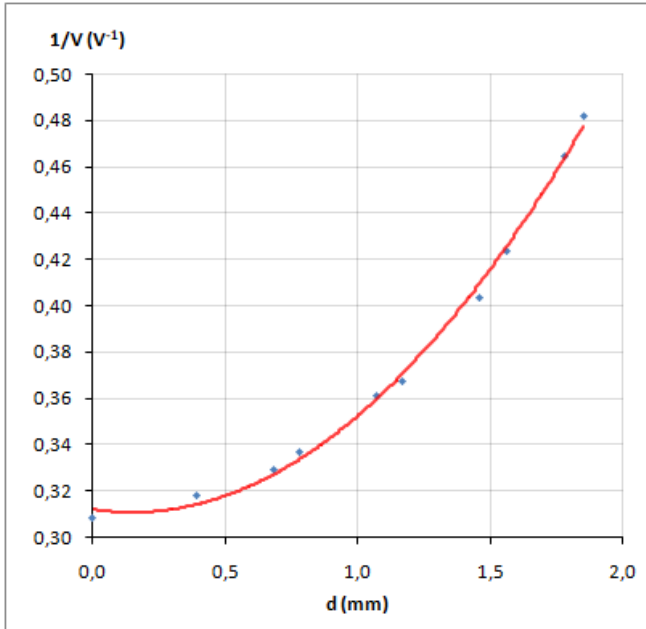


FIG. 10: In blue, the first ten points of the experimental data of FTIR. Small distances allow us to approximate the FTIR by a quadratic curve, in red. The determination coefficient of the approximation of such quadratic curve to the experimental data is $R^2 = 0.996$.

Therefore, we can approach the analysis of the experimental data sticking to the data corresponding to small distances d . On the one hand, this strengthens the quadratic approximation of the FTIR law. On the other hand, for small distances the intensity is high enough to approximate the response of the detector by a linear one: thus, experimental data does not have to be corrected for small values of d . Figure 10 shows that these approximations turn out to work properly.

IV. CONCLUSIONS

We have been able to observe and measure Total Internal Reflection (Figure 7). The fact that this was observed for 45° is consistent with the fact that the theoretical critical angle of PVC is $40.8^\circ < 45^\circ$.

Frustrated Total Internal Reflection has been also observed and measured (Figures 9 and 10). In order to compare experimental data to theoretical behaviour, several arguments and previous measures and approximations had to be made. On the one hand, the distances between the two prisms must be small (compared to λ) in order to measure FTIR. This allows to approximate the theoretical \sinh^2 law for transmittance by a quadratic law. The choice of a microwave source worked here in our favour: the greater λ , the better this approximation. On the other hand, we justified that, for small distances, the response of the detector to the incident intensity of the field can be treated as linear, allowing us to directly compare experimental data to the theoretical law. We shown that the experimental data approaches the theoretical behaviour, even under these approximations, with a determination coefficient of $R^2 = 0.996$.

Several difficulties have arisen throughout the experimental realizations of the project. Nevertheless, the phenomena behind them were interesting enough to carry a study out of them. In the first place, we have been able (Figure 5) to model the response of the detector to the field by an exponential function. Whether this is related to the fact that the detector is a rectifying diode should be more accurately studied. In the second place, we have also measured (Figure 3) the stationary waves produced between emitter and detector.

We also proved (Figure 2) has got great directionality. Nevertheless, we shown (Figure 3) that the emitted waves are not plane, since their intensity decays with distance.

Acknowledgments

I want to thank my advisor Cèsar Ferrater for his great help and his confidence in my work. I also want to acknowledge my friends Daniel del Pozo and Rosa Sánchez for their help.

-
- [1] E. Hecht, *Óptica*, (Pearson Educación, 1999, 3rd. ed.)
 [2] B. Ellis, R. Smith *Polymers: A Property Database*, (CRC Press, 2008, 2nd. ed.).
 [3] S. Zhu, A. W. Yu, D. Hawley, R. Roy, *FTIR: A demon-*

- stration and review*, 1985.
 [4] PASCO, *Complete Microwave Optics System Experiment Guide WA-9314C and WA-9314C*.